Electrochimica Acta 108 (2013) 749–756

Contents lists available at SciVerse ScienceDirect

Electrochimica Acta

journal homepage: www.elsevier.com/locate/electacta

Influence of synthesis technique on the structural and electrochemical properties of "cobalt-free", layered type $Li_{1+x}(Mn_{0.4}Ni_{0.4}Fe_{0.2})_{1-x}O_2$ $(0<x<0.4)$ cathode material for lithium secondary battery

K. Karthikeyan[a,c], S. Amaresh[a], S.H. Kim[a], V. Aravindan[a,b], Y.S. Lee[a,*]

[a] Faculty of Applied Chemical Engineering, Chonnam National University, Gwang-ju 500-757, South Korea
[b] Energy Research Institute @ NTU (ERI@N), Nanyang Technological University, Singapore 637553, Singapore
[c] Department of Mechanical and Materials Engineering, University of Western Ontario, London, Ontario, N6A 5B9, Canada

ARTICLE INFO

Article history:
Received 1 February 2013
Received in revised form 22 June 2013
Accepted 25 June 2013
Available online xxx

Keywords:
Lithium-ion batteries
Mixed hydroxide method
Layered materials
Cobalt-free cathode

ABSTRACT

We report the influence of synthesis techniques on the structural and electrochemical behavior of cobalt-free, low-cost and eco-friendly layered type $Li_{1+x}(Mn_{0.4}Ni_{0.4}Fe_{0.2})_{1-x}O_2$ $(0<x<0.4)$ cathodes for Li-ion batteries. Layered phase, $Li_{1+x}(Mn_{0.4}Ni_{0.4}Fe_{0.2})_{1-x}O_2$ $(0<x<0.4)$ was prepared by sol–gel, co-precipitation, acetate precipitation and mixed hydroxide method and by subsequent sintering at 700 °C under oxygen flow. X-ray diffraction experiments revealed the presence of α-$NaFeO_2$ type structure with $R\bar{3}m$ space group in the prepared materials. Among the layered phase compounds, material prepared by mixed hydroxide method delivered maximum reversible capacity of 207 mAh g^{-1} at current density of 0.1 mA cm^{-2} between 2 and 4.5 V *vs.* Li with excellent capacity retention characteristics as well. In addition, influence of "*x*" on electrochemical properties of $Li_{1+x}(Mn_{0.4}Ni_{0.4}Fe_{0.2})_{1-x}O_2$ $(0<x<0.4)$ were also investigated and such samples were prepared by mixed hydroxide route.

1. Introduction

Due to the depletion in the levels of fossil fuels and an increase in environmental awareness, there are many efforts being devoted to find out suitable alternative energy sources, especially automobile applications. Lithium-ion batteries (LIB) are considered as one of the promising energy storage devices because of their high volumetric and gravimetric energy density with light weight and shape versatility; these properties have already engaged them in many potential portable applications like laptops, cameras, mobile phones, furthermore they are expected to power electric vehicles (EV) and hybrid electric vehicles (HEV) in near future [1–5]. Layered $LiCoO_2$ has been dominated as a cathode material since the commercialization of LIBs by Sony because of stable discharge plateau, high working voltage and long cycle life [1,6]. However, the possibility of employing them in high power applications such as EV and HEV is highly restricted due to the structural instability, while approaching beyond 0.5 moles of Li (>4.3 V *vs.* Li), high cost, safety, and toxicity [1]. Therefore, alternate cathodes like $Li(Mn,Ni)O_2$ and $LiMn_2O_4$ have been proposed and extensively studied as prospective candidates to replace $LiCoO_2$ [7–9], for example $LiNiO_2$ has been demonstrated to deliver higher reversible capacity, but is associated with poor thermal stability and difficulty in synthesizing a phase pure structure. On the other hand, $LiMn_2O_4$, which possesses higher thermal stability than layered compounds, demonstrates its inapplicability for use in LIBs due to lower reversible capacity with operating potential of ~4 V *vs.* Li and poor cycleability at elevated conditions. To overcome these disadvantages, intensive research work has been carried out to develop the derivatives like $LiNi_{1/2}Mn_{1/2}O_2$ and $LiNi_{1/3}Mn_{1/3}Co_{1/3}O_2$ with α-$NaFeO_2$ crystal structure [10]. In spite of delivering high capacity, low rate capability of those derivatives are inevitable and also the significant cation disorder between the lithium and transition metal ions slabs are another important concern for such phases [11–16]. Despite the high rate performance and high operating voltages of layered and spinel oxides and their derivatives, the observed reversible capacities make them inappropriate to be employed in EV and HEV applications. On the other hand, polyanion framework materials, *i.e.* $LiFePO_4$ rendered good thermal stability in both lithiated and de-lithiated states, however operating potential was restricted to ~3.4 V *vs.* Li, which resulted in less energy density. Rest of the polyanion group olivine phase materials like, $LiMnPO_4$ and $LiCoPO_4$ are not completely recognized to be employed as prospective cathodes due to their own setbacks [1,17,18]. Recently, Tabuchi et al. [19,20] have reported iron substituted

* Corresponding author. Tel.: +82 62 530 1904; fax: +82 62 530 1904.
E-mail addresses: aravind_van@yahoo.com (V. Aravindan), leeys@chonnam.ac.kr (Y.S. Lee).

0013-4686/$ – see front matter © 2013 Elsevier Ltd. All rights reserved.
http://dx.doi.org/10.1016/j.electacta.2013.06.142

Li_2MnO_3 ($Li_{1+x}(Fe_yMn_{1-y})_{1-x}O_2$, $0 \le x \le 1/3$, $0.3 \le y \le 0.7$) layered material as new class of cathode materials for LIB applications. Unfortunately, the operating potential of these materials is too low and the delivered discharge capacity lower than 80 mAh g^{-1}. Later, the same group proposed series of nickel and iron containing layered solid-solution of Li_2MnO_3 ($Li_{1+x}[(Fe_{1/2}Ni_{1/2})_yMn_{1-y}]_{1-x}O_2$, $0 < x < 1/3$, $0.2 \le y \le 0.8$) with an average discharge voltage of 3.5 V *vs.* Li. Nevertheless, such system experienced a severe capacity fade during cycling, which was mainly due to the complex synthetic procedures involved in the preparation of such single phase material. As a result of which, inferior electrochemical properties of the compounds were observed [21]. In order to improve the electrochemical properties of the solid-solutions of Li_2MnO_3, several approaches have been employed [13]. In our previous work, we successfully reported the synthesis and performance of "cobalt-free" $Li_{1.2}Mn_{0.32}Ni_{0.32}Fe_{0.16}O_2$ ($x = 0.2$) with three end members of Li_2MnO_3, $LiNiO_2$ and $LiFeO_2$ by simple sol–gel technique in the presence of various concentrations of adipic acid [22]. However, such compounds have experienced poor rate performance, which is one of the prerequisite for HEV and EV applications. In this connection, we attempted to study the influence of synthesis technique on the electrochemical performance of $Li_{1+x}(Mn_{0.4}Ni_{0.4}Fe_{0.2})_{1-x}O_2$ ($x = 0.2$) cathodes prepared by various approaches like sol–gel (SG), co-precipitation (CP), acetate precipitation (AP) and mixed hydroxide (MH) methods. The effect of preparation method on the structural and electrochemical properties have been extensively evaluated and presented in this work. Further, the influence of transition metal concentration was also investigated ($0 < x < 0.4$) by MH route and described in detail.

2. Experimental

All analytical grade starting materials like, $Li(CH_3COO)_2{\cdot}H_2O$ (Wako, 99.9%), $Fe(CH_3COO)_2{\cdot}H_2O$ (Sigma–Aldrich, 99.99%)), $Ni(CH_3COO)_2{\cdot}4H_2O$ (Sigma–Aldrich, 99.9%)), $Mn(CH_3COO)_2{\cdot}4H_2O$ (Sigma–Aldrich, 99.99%)), LiOH (Jensei Chemicals, 95%) $Fe(NO_3)_3{\cdot}9H_2O$ (Jensei Chemicals, 98%), $MnCl_2{\cdot}4H_2O$ (Wako, 99.9%), $Ni(NO_3)_3{\cdot}6H_2O$ (Jensei Chemicals, 97%), Na_2CO_3 (Sigma–Aldrich, 99%) and acetic acid were procured and used as such without any further purification. For the preparation of $Li_{1.2}Mn_{0.32}Ni_{0.32}Fe_{0.16}O_2$ ($x = 0.2$) phase by CP, two aqueous solutions *viz.* 0.2 M Na_2CO_3 solution, transition-metal precursor solutions with a concentration of 0.1 M for each metal precursor ($MnCl_2$, $Fe(NO_3)_3$, and $Ni(NO_3)_3$) were prepared. Metal precipitate was obtained by mixing of carbonate solution into the transition metal solution and the solution pH was adjusted to 11 using $NH_3OH{\cdot}H_2O$ solution. Subsequently, the solution was continuously stirred at 60 °C for 6 h. Resultant $(Mn_{0.32}Ni_{0.32}Fe_{0.16})CO_3$ precipitate was filtered, washed with distilled water and dried over night at 80 °C. The final product was obtained by mixing $(Mn_{0.32}Ni_{0.32}Fe_{0.16})CO_3$ with appropriate amount of LiOH and the mixture was heated to 400 °C for 4 h, and then fired at 700 °C for 10 h in oxygen atmosphere to yield the $Li_{1.2}Mn_{0.32}Ni_{0.32}Fe_{0.16}O_2$ ($x = 0.2$) solid solution.

The $MnCl_2$, $Fe(NO_3)_3$ and $Ni(NO_3)_3$ were used as starting materials for preparing the AP technique, in which acetic acid acted as the precipitating agent to yield the precursor power. Then the precursor powders were mixed with appropriate amount of LiOH and calcined by the procedure described above. In the case of SG procedure, the powders were synthesized by following our previously described method, but without using chelating agent [22].

Finally, $(Li_{1+x}(Mn_{0.4}Ni_{0.4}Fe_{0.2})_{1-x}O_2$ ($0 < x < 0.4$) materials were also prepared by the MH method with different x value followed by calcination at 700 °C under oxygen atmosphere. In a typical synthesis, 0.125 M of $MnCl_2$, $Fe(NO_3)_3$, and $Ni(NO_3)_3$ metal salts were dissolved in distilled water and then appropriate stoichiometric amount of aqueous LiOH solution was added to the metal solution to obtain mixed hydroxide precipitates and further aged overnight. Subsequently, the precipitate was filtered, washed to remove residual Li salts and dried at 60 °C for 10 h. The final products were obtained by firing the precipitates with slight excess of LiOH at 700 °C for 10 h under oxygen flow. The same procedure was followed to prepare the samples with different x values. The final products prepared with $x = 0.2$ using CP, AP, SG and MH at 700 °C were labeled as CP2T700, AP2T700, SG2T700 and MH2T700, respectively. The materials synthesized with $x = 0$, 0.1, 0.3 and 0.4 at 700 °C through MH method were named as MH0T700, MH1T700, MH3T700 and MH4T700, respectively.

Table 1
Lattice contents of $Li_{1.2}Mn_{0.32}Ni_{0.32}Fe_{0.16}O_2$ ($x = 0.2$) solid solutions prepared using different synthesis methods.

Sample	a_h (nm)	c_h (nm)	c/a	I_{003}/I_{104}
SG2T700	2.889	14.289	4.95	1.12
CP2T700	2.891	14.285	4.95	0.75
AP2T700	2.887	14.277	4.95	0.77
MH2T700	2.881	14.276	4.94	0.98

Phase purity and structural properties of the synthesized materials were analyzed by X-ray diffraction (XRD) measurements using Rint 1000 Rigaku, Japan equipped with Cu Kα radiation. Surface morphologies of the powders were examined by SEM images (S-4700 microscope, Hitachi, Japan). Brunauer–Emmett–Teller (BET) surface area was analyzed through a Micromeritics ASAP 2010 surface area analyzer (Micromeritics, USA). The crystal structures of the prepared powders were also confirmed by micro-Raman spectrometer (LabRam HR 800, France) with holographic gratings. All the electrochemical characterizations were carried out using standard 2032-type coin cell configuration. For the fabrication of composite cathode, 20 mg of prepared material was mixed with 3 mg of Ketzen black and 3 mg of teflonized acetylene black (TAB-2) using ethanol. The slurry was pressed on 200 mm^2 nickel mesh current collector and dried at 160 °C for 4 h. Test cells comprised of composite cathode and lithium foil anode, which were separated by porous polypropylene film separator (Celgard 3401) and filled with 1 M $LiPF_6$ (1:1 ethylene carbonate/dimethyl carbonate, Techno Semichem Co., Ltd., Korea) electrolyte solution. The entire cell-assembly process was carried out in an argon-filled glove box. These cells were galvanostatically charged and discharged at various current densities between 2 and 4.5 V *vs.* Li at ambient temperature.

3. Results and discussion

The XRD patterns of $Li_{1.2}Mn_{0.32}Ni_{0.32}Fe_{0.16}O_2$ phase prepared with different synthesis techniques at 700 °C are presented in Fig. 1a. It can be seen from Fig. 1a, that all the samples exhibit phase-pure layered structure without any traces of impurities. In addition, XRD peaks observed between 20° and 30° corresponds to the super lattice ordering of Li and transition metal containing layers which is correlated to the dominance of Li_2MnO_3 end member [13–16]. Moreover, the SG2T700 and CP2T700 powders exhibited shoulder like reflections for *hkl* planes of (1 0 1) and (1 0 4), whereas the materials prepared through AP and MH methods showed quite narrow peaks. The disappearance of shoulder like peaks indicate that the powders prepared through AP and MH route comprised the mixture of monoclinic and hexagonal layered phase [21]. The XRD patterns are indexed based on α-$NaFeO_2$-type structure with $R\bar{3}m$ space group, which has the basic Mn(Ni)—O—Mn(Ni)···linkage units that formed the layered component [23]. The lattice parameters values are calculated from the XRD data and listed in Table 1. In Table 1, small variation in the lattice parameter values can be

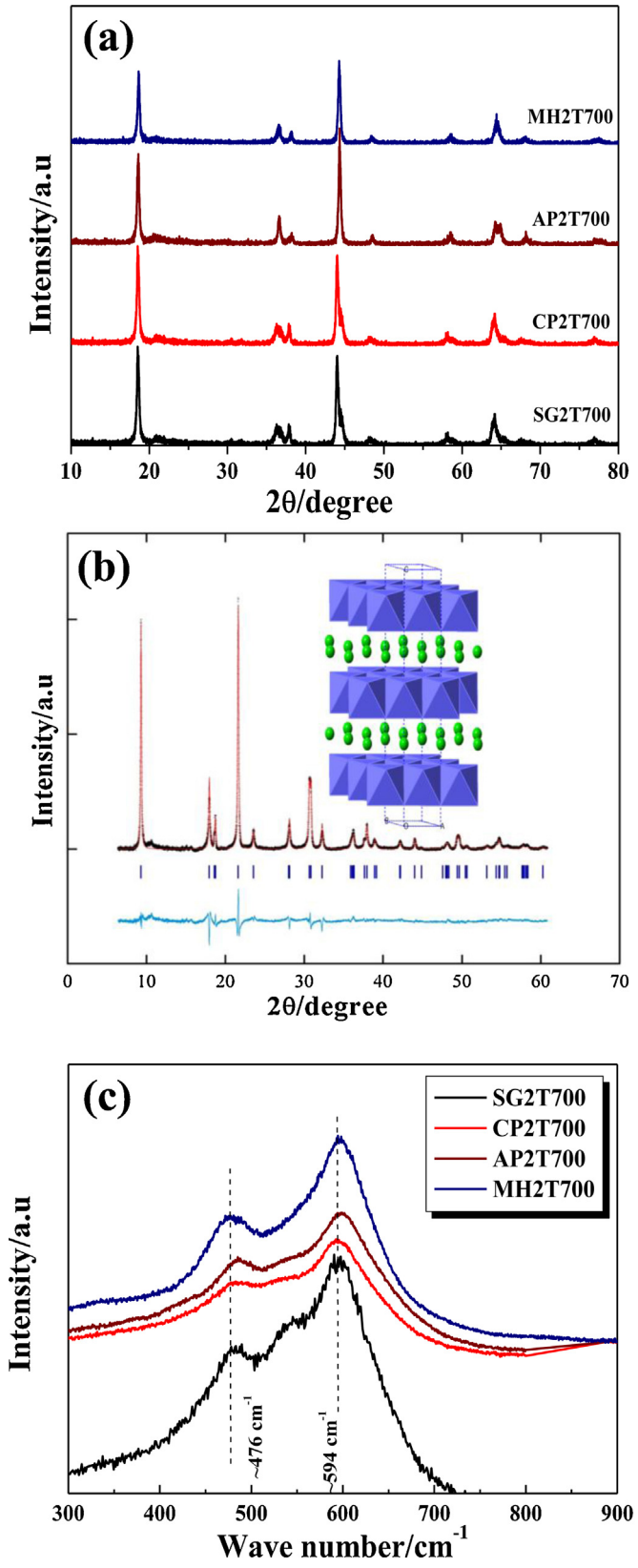

Fig. 1. (a) XRD patterns of $Li_{1.2}Mn_{0.32}Ni_{0.32}Fe_{0.16}O_2$ synthesized using different methods at 700 °C in oxygen atmosphere. (b) Rietveld refinement of MH2T700 powders calcined at 700 °C in oxygen atmosphere. The refinement parameters and the α-$NaFeO_2$ type crystal structure ($R\bar{3}m$) are shown in inset and (c) Raman spectra of the powers prepared with SG, CP, AP and MH methods.

Table 2
ICP of $Li_{1.2}(Mn_{0.32}Ni_{0.32}Fe_{0.16})O_2$ prepared at different methods.

Elements	SG2T700	MH2T700	CP2T700	AP2T700
Li	1.11	1.15	1.09	1.14
Mn	0.320	0.319	0.321	0.320
Fe	0.164	0.158	0.159	0.162
Ni	0.327	0.317	0.324	0.316

observed from one synthesis technique to another. It is well known that, when the *c/a* ratio is higher than 4.9 the material posses predominantly layered characteristics [24]. In the present case, the *c/a* ratio of all the materials was higher than 4.9, which clearly indicates the preparation of materials with excellent layered structure characteristics. Intensity ratio of $I_{(003)}/I_{(104)}$ is another sensitive parameter to measure the cation disordering between Li and transition metal layers [23,24]. It is apparent from Table 1, that the $I_{(003)}/I_{(104)}$ ratio for MH2T700 sample is around unity, which indicates almost negligible cation mixing and this result is in good agreement with other reports [1,25,26]. Therefore, a good electrochemical performance is expected for the sample synthesized using MH method. Furthermore, as per the Table 1, there might be occurrence of fractional cation disordering between Ni and Li, but not significant when compared to rest of the synthesis approaches. In order to find out the cation disordering in sample prepared with MH method, the XRD pattern of MH2T700 was examined by Rietveld refinement and provided in Fig. 1b. The refinement was carried out based on the assumption that occupancy of Li-ions in 3*a* site; transition metal ions in 3*b* site and O atoms in 6*c* site and corresponding crystal structures based on α-$NaFeO_2$ type with $R\bar{3}m$ space group. The typical crystal structure is given as inset in Fig. 1b. It has been reported that lithium ions and transition metal ions occupy alternating layers in a cubic close packed framework of oxygen, which correspond to 3*a* and 3*b* site [27]. The ICP analysis is also carried out to ensure the composition of the elements present in the compounds (given in Table 2). According to Rietveld analysis, only 0.06 unit mole of Ni^{2+} from 3*b* site incorporates into the lithium layer giving a final composition of $(Li_{0.940}\ Ni^{2+}{}_{0.06})_{3a}(Li_{0.260}, M_{0.740})_{3b}O_2$, where M stands for transition metals (Mn, Ni and Fe) whereas 0.08 unit mole of Ni^{2+} is intercalated for SG prepared phases. This report clearly reveals that only lower amount of cation disordering occurred in the case of MH2T700 sample.

The Raman spectrum was also employed to substantiate XRD results for layered compounds prepared by abovementioned process. Raman spectra of the sample prepared with different synthesis method are presented in Fig. 1c. In the case of layered compounds, Raman active modes are generally observed between 400 and 650 cm^{-1}, which are related to the M—O and O—M—O bending modes originated from the vibration of oxygen atoms [28,29]. In the present study, the peaks observed at 476 and 594 cm^{-1} for all the samples represent the Raman-active species of E_g and $A1_g$ modes, respectively. The oscillation strength of $A1_g$ mode exhibited higher intensity (approximately two times) than that of E_g mode [29]. In addition, the shifting of peak position toward higher frequency region for MH2T700 sample indicates the expansion of inter-slab distance, which promotes facile lithium ion diffusion during electrochemical cycling, especially at high current rates [30].

The SEM images of $Li_{1.2}Mn_{0.32}Ni_{0.32}Fe_{0.16}O_2$ samples prepared by different methods are given in Fig. 2. The SG2T700 and CP2T700 samples exhibited uneven sized particulate morphology with severe agglomeration. It can be seen from Fig. 2c, that for AP2T700 sample, the particles showed flake like morphology and were arranged one over another, which formed bigger crystals. In the case of MH2T700 (Fig. 2d), the powders exhibited almost cubic shaped particles with sharp edges and uniform size distribution (particle size ~60–100 nm). BET surface area of the powders were

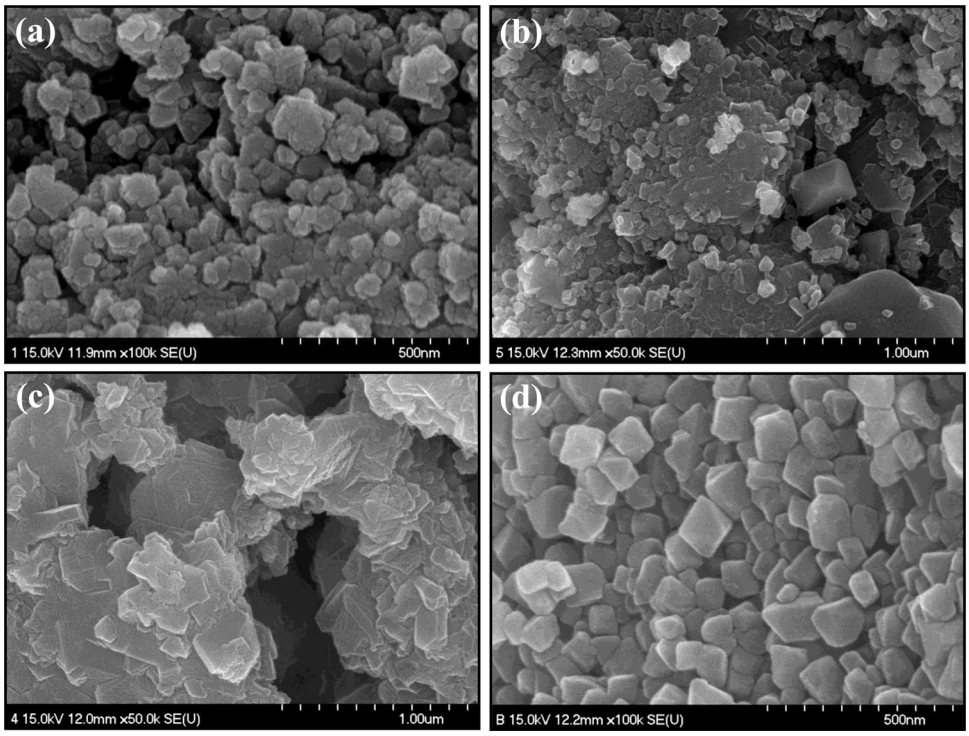

Fig. 2. SEM images of (a) SG2T700, (b) CP2T700, (c) AP2T700 and (d) MH2T700 powders prepared at 700 °C under oxygen flow, respectively.

also measured and found to be 4.44, 5.03, 12.05 and 20.17 $m^2\,g^{-1}$ for SG2T700, CP2T700, AP2T700 and MH2T700 powders, respectively. It is well known that, electronic transport properties of the materials also depend on the morphological features, therefore smaller size with higher surface area particles are favorable for facile diffusion of Li-ions during electrochemical studies [31].

Cyclic voltammetric (CV) studies were conducted for $Li_{1.2}(Mn_{0.32}Ni_{0.32}\ Fe_{0.16})O_2$ powders prepared by different synthesis routes in half-cell configuration between 2 and 4.5 V *vs.* Li at scan rate of 0.2 $mV\,s^{-1}$ are represented in Fig. 3. It can be seen from Fig. 3, that all the samples exhibit one major oxidation peak at ~4.2 V *vs.* Li during charge and at ~3.6 V *vs.* Li during discharge process. The presence of such peaks is attributed to the Ni^{2+}/Ni^{4+} redox couple [22,26] and it is worth mentioning here that, in order to maintain the charge neutrality the presence of Ni ions with oxidation state of 2+ is plausible in $Li_{1.2}(Mn_{0.32}Ni_{0.32}\ Fe_{0.16})O_2$

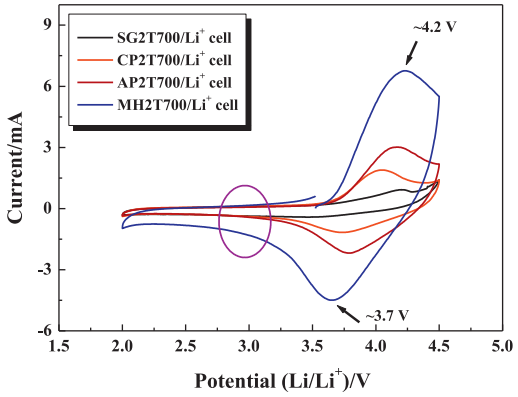

Fig. 3. CV traces of the test cell containing $Li_{1.2}Mn_{0.32}Ni_{0.32}Fe_{0.16}O_2$ electrodes synthesized using SG, CP, AP and MH methods in half-cell configuration between 2 and 4.5 V *vs.* Li at scan rate of 0.2 $mV\,s^{-1}$. Metallic lithium acts as both counter and reference electrode during CV measurements.

phase [32,33]. Furthermore, the absence of redox peak at ~3 V *vs.* Li suggests that Mn ions are electrochemically inactive, which clearly indicates the presence of Mn in 4+ state [34]. As expected, the shift in Li-extraction potential toward lower voltage was noted for CP2T700 sample (~4.05 V *vs.* Li), which was presumably due to severe cation mixing. Consequently, MH2T700 powder exhibited a stronger current response during both anodic and cathodic sweeps than rest of the materials prepared by different synthetic routes. The higher current response of MH2T700 originated from the smaller particle size with large exposed surface area, negligible cation mixing and good contact toward current collectors, which facilitated Li-ion diffusion during charge–discharge process thereby resulting in enhanced electrochemical behavior [1,31].

Fig. 4a represents the typical galvanostatic charge–discharge curves of the samples prepared by different synthesis techniques. The cycling studies were conducted between 2 and 4.5 V *vs.* Li at current density of 0.1 $mA\,cm^{-2}$ in ambient temperature. It is well known that the Mn^{4+} cannot participate in the electrochemical reaction due to its oxidation state, since the redox couple of $Mn^{4+/5+}$ is not electrochemically possible [13–16,34]. Furthermore, it is obvious from the charge–discharge curves, that the absence of a redox couple around 4 V *vs.* Li in indicates non-involvement of Fe^{3+} in the electrochemical reaction, which is consistent with the CV analysis [21,22]. Hence, the capacity is obtained by $Ni^{2+/4+}$ redox couple, which is only possible *via* Ni^{3+} is assumed to be formed during the testing range, which is in good agreement with the CV studies [33]. This clearly demonstrates that the Mn^{4+} and Fe^{3+} are electrochemically inactive and involved only for stabilizing the crystal structure of $Li_{1.2}(Mn_{0.32}Ni_{0.32}Fe_{0.16})O_2$ during the charge–discharge process [21,22]. All the samples exhibited a smooth discharge curves until 3.5 V *vs.* Li and a flat plateau was observed around 2.25–2 V *vs.* Li. However, the appearance of such a gradient is not well understood and it is worth mentioning that a similar kind of trend was also noticed by Tabuchi et al. [20]. Among the cells tested, MH2T700-based cell showed very low irreversible capacity loss (ICL) *ca.* 10% when compared to

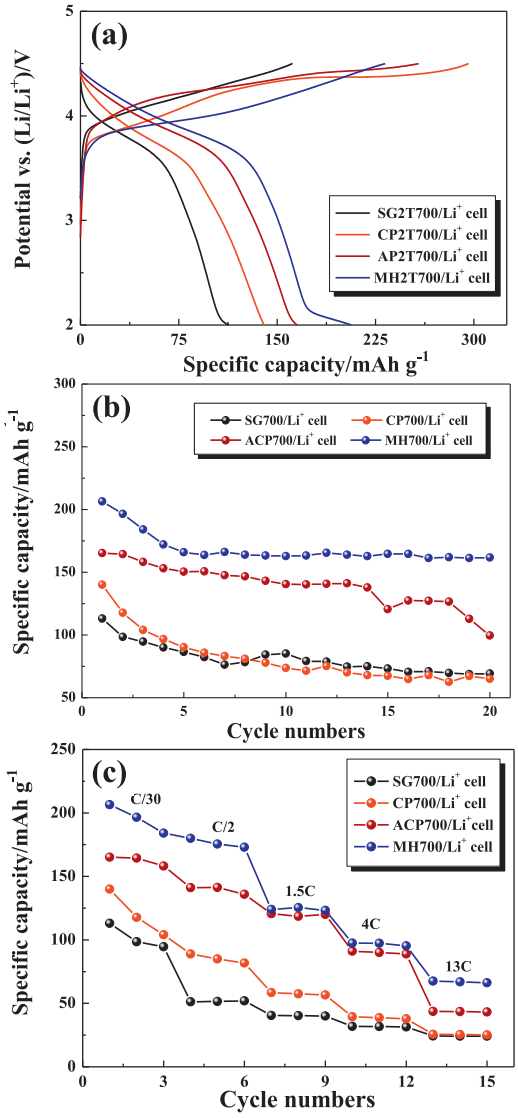

Fig. 4. (a) The initial charge discharge curves of SG2T700, CP2T700, AP2T700 and MH2T700 cells in half-cell configuration and tested between 2 and 4.5 V *vs.* Li at constant current density of 0.1 mA cm^{-2}. (b) Plot of discharge capacity *vs.* cycle number for $Li_{1.2}Mn_{0.32}Ni_{0.32}Fe_{0.16}O_2$ electrodes prepared by different synthesis methods and (c) rate performance of the test cells at different current rates from C/30 to 13 C.

rest of the materials. The possible reason for such a huge ICL is due to the presence of Ni^{2+} ions occupying the active Li-sites, which subsequently prevents the re-insertion of Li-ions during discharge process. The discharge capacity of 113, 140, 165 and 207 mAh g^{-1} was observed for SG2T700, CP2T700, AP2T700 and MH2T700 powders, respectively. Apparently, discharge capacity of the sample prepared by MH method was higher when compared to the others synthesis routes employed. Consequently, poor structural and morphological features of SG2T700 and CP2T700 samples resulted in less initial capacity. Fig. 4b shows the cycling profiles of $Li_{1.2}(Mn_{0.32}Ni_{0.32}\ Fe_{0.16})O_2$ powders prepared with different methods at a constant current density of 0.1 mA cm^{-2}. The test cells retained 46%, 62%, 60% and 88% of initial reversible capacity for SG2T700, CP2T700, AP2T700 and MH2T700 powders, respectively. Amongst all the samples, MH2T700 sample showed excellent electrochemical behavior when compared to rest of the synthesis routes adopted. Apart from higher capacity, high rate performance is also one of the important criteria to be employed to function as a cathode material in LIB. For the rate performance

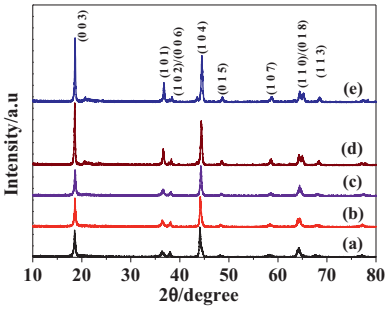

Fig. 5. XRD patterns of $Li_{1+x}(Mn_{0.4}Ni_{0.4}Fe_{0.2})_{1-x}O_2$ ($0 < x < 0.4$) prepared by mixed hydroxide method with different x value at 700 °C under oxygen atmosphere (a) 0, (b) 0.1, (c) 0.2, (d) 0.3 and (e) 0.4, respectively.

studies, no alterations in the composition of the electrodes were made. The rate performance of the electrode materials prepared with different synthesis procedure at various current densities ranging from C/30 to 13 C with the potential range between 2 and 4.5 V *vs.* Li are presented in Fig. 4c. Linear decrease in capacity profiles were noted with an increase in current rate irrespective of the synthesis procedures employed. As expected, rate capability and capacity profiles of MH2T700 electrode was higher than that of other materials tested. The rate performance data clearly supports the influence of synthesis method on the electrochemical performances. The improved cycling behavior and rate performance of MH2T700 electrode is attributed to the (i) smaller and uniform sized particles with even distribution, (ii) relatively larger surface area, (iii) negligible amount of cation mixing and (iv) its superior structural integrity provided by Fe^{3+} ions in the layered matrix. Importantly, small sized particles with larger surface area not only bestow higher electrode/electrolyte interface for electrochemical reaction, but also increases better contact toward current collector and thereby increases lithium ion diffusion properties and conductivity profiles as well [1,13,31]. This enhanced electrochemical performance of MH2T700 clearly reflects/supports the results observed from the SEM, BET and Raman analysis.

Apparently, MH route is one of the efficient techniques to produce high performance layered type electrode materials for LIB. Excellent battery performance obtained from our previous results for the development of eco-friendly and Fe containing layered type materials by adipic acid assisted sol–gel technique and present work with $Li_{1+x}(Mn_{0.4}Ni_{0.4}Fe_{0.2})_{1-x}O_2$, $x = 0.2$, which motivated us to study the influence of metal concentration [22]. Therefore, we are very keen to alter the composition of cathodes to study its influence while approaching other synthetic routes. In other words, influences of x value on the electrochemical performance were investigated by adopting the mixed hydroxide process to attain the desired phase. Fig. 5 shows the XRD patterns of $Li_{1+x}(Mn_{0.4}Ni_{0.4}Fe_{0.2})_{1-x}O_2$ ($0 < x < 0.4$) powders prepared using MH method at 700 °C under oxygen flow. All XRD reflections were similar to $Li_{2-x}MnO_{3-x/2}$ (α-$NaFeO_2$ with $R\bar{3}m$ space group) rather than nearly stoichiometric Li_2MnO_3 (monoclinic $C_{2/m}$) phases without any traces of impurities. The sub-lattice of oxygen in α-$NaFeO_2$ formed a closed pack face centered lattice in c direction resulting in a clear splitting of hexagonal doublet peaks [33]. Generally, if there is no distortion, doublet reflection merges into a single peak. From Fig. 5, it is clear that the splitting of (0 0 6)/(0 1 2) and (1 0 8)/(1 1 0) is more evident indicating an increase in the hexagonal ordering of the material with an increase in x value. It should be noticed here that the $(I_{(006)} + I_{(102)}/I_{(101)})$ ratio is decreased with x concentration indicating that the material has low cationic disordering, which promotes the electrochemical performance [35]. The lattice parameters of samples were calculated and listed in Table 3 and found that values were increased linearly with an increase in x value.

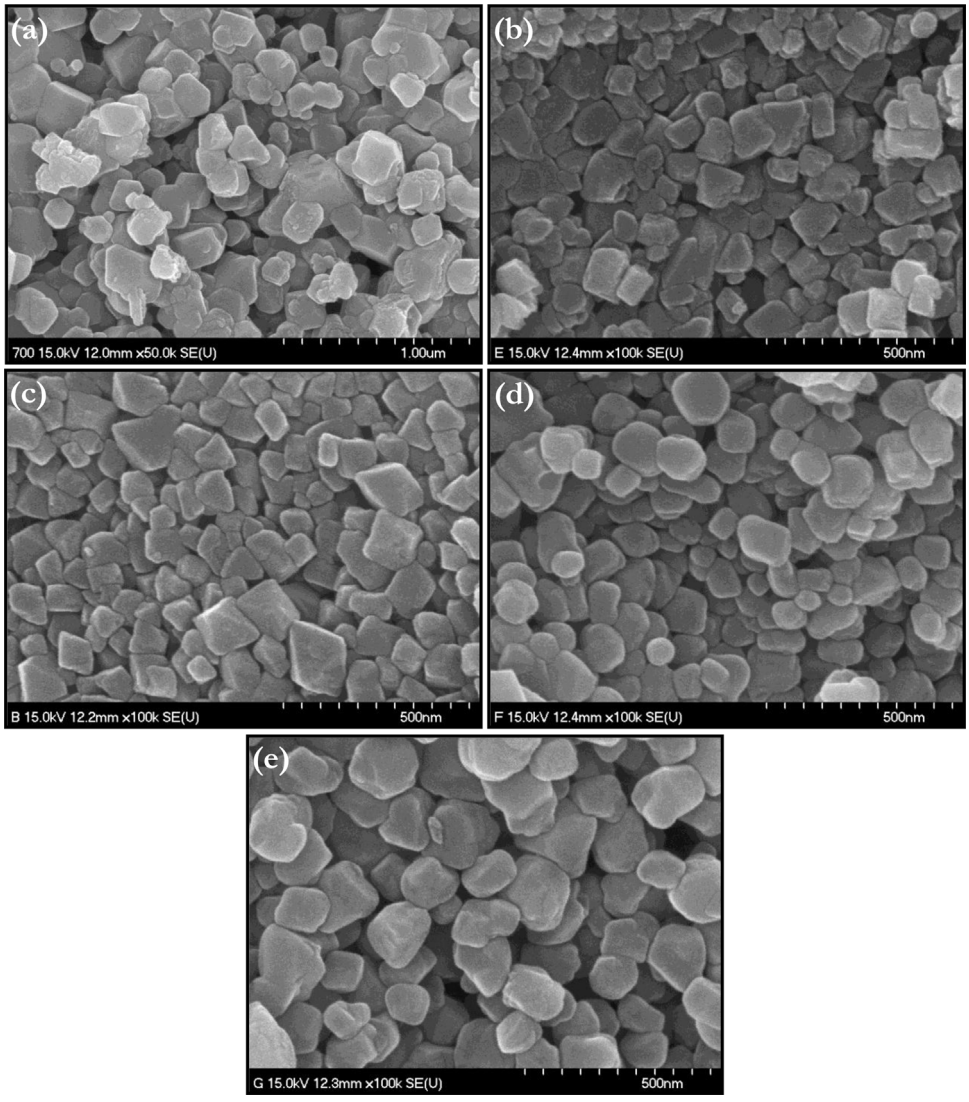

Fig. 6. SEM images of $Li_{1+x}(Mn_{0.4}Ni_{0.4}Fe_{0.2})_{1-x}O_2$ $(0 < x < 0.4)$ powders obtained by mixed hydroxide method with different x value (a) 0, (b) 0.1, (c) 0.2, (d) 0.3 and (e) 0.4, respectively.

This difference in lattice parameter revealed that the samples were prepared with different structural integrity because lattice parameter is closely related with atomic distribution. It can be seen from Table 3, that MH4T700 sample exhibits the highest $I_{(003)}/I_{(104)}$ ratio, *i.e.* lower cation mixing, which could be considered as quite beneficial for better lithium ion insertion/extraction reaction, whereas MH0T700 sample showed the least value. Moreover, value of *c/a* was higher than 4.9 for all the samples, which is the typical characteristic signature of the materials with layered structure [24]. The ICP analysis is also carried out to ensure the composition of the elements in the compounds (given in Table 4).

Scanning electronic microscopic (SEM) images of $Li_{1+x}(Ni_{0.4}Mn_{0.4}Fe_{0.2})_{1-x}O_2$ $(0 < x < 0.4)$ samples are presented in Fig. 6. All the samples exhibited similar kind of particulate morphology with sharp edges and uniform distribution of the particles. Gradual increase in the particle size from 70 to 125 nm was noted with an increase in the x value. The increase in particle size is known to originate from the higher lithium content, which enhances particle growth during synthesis process [19–21,33].

Typical galvanostatic charge–discharge curves of $Li_{1+x}(Mn_{0.4}Ni_{0.4}Fe_{0.2})_{1-x}O_2$ $(0 < x < 0.4)$ phase materials in half-cell configurations were cycled between 2 and 4.5 V *vs.* Li at current density of 0.1 mA cm^{-2} and presented in Fig. 7a. It can be seen from Fig. 7a, that the charge and discharge capacities of the samples are linearly increased with an increase in x value 0.2 and tend to decrease beyond 0.2 content (Fig. 7b). Not only variation in the

Table 3
Lattice parameter values of $Li_{1+x}(Mn_{0.4}Ni_{0.4}Fe_{0.2})_{1-x}O_2$ $(0 < x < 0.4)$ powders synthesized through MH method at 700 °C with different x values.

Sample	a_h (nm)	c_h (nm)	c/a	I_{003}/I_{104}
MH0T700	2.864	14.259	4.93	0.92
MH1T700	2.873	14.265	4.94	0.94
MH2T700	2.881	14.276	4.94	0.98
MH3T700	2.893	14.287	4.95	1.04
MH4T700	2.899	14.292	4.95	1.10

Table 4
ICP of $Li_{1+x}(Mn_{0.4}Ni_{0.4}Fe_{0.2})_{1-x}O_2$ $(0 < x < 0.4)$ powders synthesized through MH method with different x values at 700 °C.

Elements	MH0T700	MH1T700	MH2T700	MH3T700	MH4T700
Li	0.98	1.06	1.15	1.26	1.34
Mn	0.398	0.359	0.319	0.279	0.237
Fe	0.199	0.179	0.158	0.141	0.119
Ni	0.397	0.362	0.317	0.281	0.24

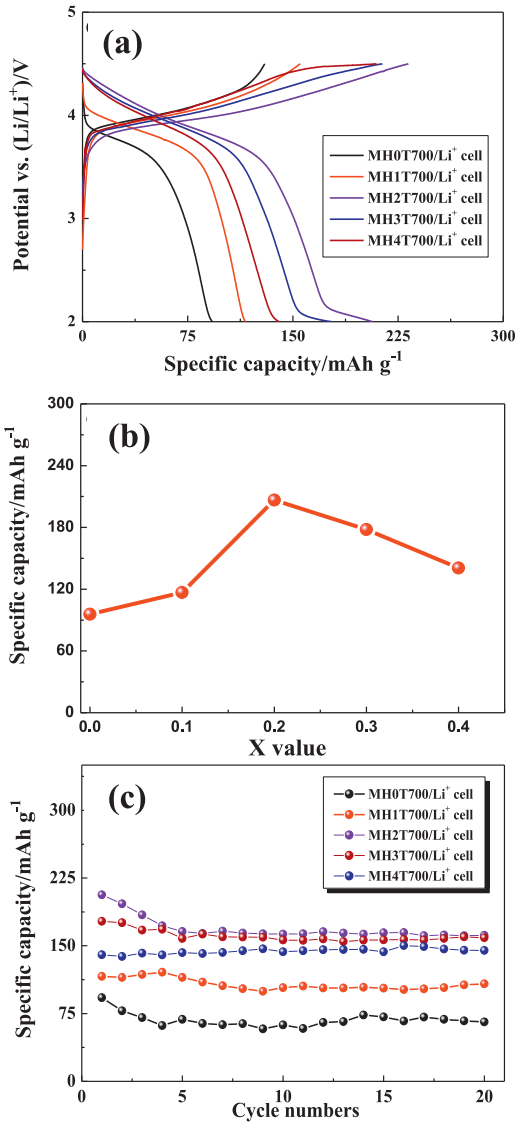

Fig. 7. (a) Galvanostatic charge–discharge curves of the $Li_{1+x}(Mn_{0.4}Ni_{0.4}Fe_{0.2})_{1-x}O_2$ ($0 < x < 0.4$) samples with different x value at current density of 0.1 mA cm^{-2} between 2 and 4.5 V *vs.* Li and (b) plot of discharge capacity *vs.* cycle number.

specific capacities, also variation in OCV is evident from the Fig. 7a. This variation in OCV is mainly due to the hexagonal ordering of the layered compound, which substantially provides necessary conductivity to enable higher potential [36]. Therefore, similar kind of variation in the electrochemical trends are anticipated and evidenced from the Fig. 7b. The influence of x content on the electrochemical properties of the solid-solution, particularly during discharge process is evident from Fig. 7b. An additional discharge plateau at ~2.25 V *vs.* Li is observed for the concentration of $x = 0.2$, 0.3 and 0.4 only, which is not detected for the samples with lower x concentrations [37,38]. The test cells delivered initial discharge capacities of 93, 117, 207, 179 and 143 mAh g^{-1} for MH0T700, MH1T700, MH2T700, MH3T700 and MH4T700 powders, respectively. This may be due to the morphological effect of the materials, since size of the particles directly influences the Li-diffusion properties [22,27,31]. Fig. 7c represents the cycling performance of samples prepared with different x value at ambient temperature conditions. Irrespective of the x content, a meager amount of capacity fading was noted during the cycling process. As expected, MH2T700 powder exhibited higher cycleability than rest of the prepared concentrations which indicates the influence of x value is found not impressive. Nevertheless, structural integrity of MH04T700 sample was found to be higher though it delivered slightly lower capacity when compared to MH2T700 powders and presented good cycleability when compared to the others, which exhibited almost negligible amount of capacity fading, whereas MH0T700 rendered poor cycle life. The rapid capacity fading of MH0T700 sample may be attributed to the formation of spinel-like oxide during the subsequent cycling and similar kind of behavior has been noted for Li_2MnO_3 and $LiCoO_2$–Li_2MnO_3 systems [39,40]. The test cells with different x content retained the initial discharge capacity of 93%, 88% and 90% for MH01T700, MH02T700 and MH03T700 powders, respectively. Importantly, highest reversible capacity of ~162 mAh g^{-1} was noted after 20 cycles for MH02T700 sample. This observation further convinces that $x = 0.2$ would be an optimum concentration to yield high performance $Li_{1+x}(Ni_{0.4}Mn_{0.4}Fe_{0.2})_{1-x}O_2$ solid-solutions in terms of higher reversible capacity, capacity retention and eco-friendliness by mixed hydroxide approach [19,20,22,41,42]. Further studies are in progress to improve the cycle life of the samples by increasing the lithium content or minimizing cubic phase formation. These results clearly demonstrated that the appropriate amount of nickel and iron substitution in layered Li_2MnO_3 phase remarkably improved the electrochemical performances of native phase to develop high capacity cathode active material with eco-friendliness and low cost to power HEV and EV applications in near future [33].

4. Conclusions

'Cobalt-free' layered type $Li_{1.2}(Mn_{0.32}Ni_{0.32}Fe_{0.16})O_2$ ($x = 0.2$) materials were synthesized using different synthesis approaches. The XRD patterns revealed the formation of layered α-$NaFeO_2$ structure with existence of super-lattice monoclinic Li_2MnO_3 phase. The $Li_{1.2}(Ni_{0.32}Mn_{0.32}Fe_{0.16})O_2$ phase prepared with mixed hydroxide method at 700 °C delivered highest reversible capacity of 207 mAh g^{-1} with good capacity retention characteristics than sol–gel, co-precipitation and acetate precipitation. The excellent performance of sample prepared by MH method was due to the smaller particle size with high specific surface area and good hexagonal ordering than other synthesis techniques employed. Furthermore, mixed hydroxide process was used to study the effect of x content on the electrochemical properties of $Li_{1+x}(Mn_{0.4}Ni_{0.4}Fe_{0.2})_{1-x}O_2$ ($0 < x < 0.4$) solid-solution. At lower concentration ($0 < x < 0.1$), test cells delivered poor electrochemical performance due to the existence of higher amount of Li_2MnO_3 content. On the other hand, MH4T700 sample exhibited good capacity retention characteristics because of the structural integrity provided by Mn^{4+} and Fe^{3+} ions. This study brings forth the information that, $Li_{1+x}(Ni_{0.4}Mn_{0.4}Fe_{0.2})_{1-x}O_2$ ($0 < x < 0.4$) solid-solution containing inexpensive Ni, Mn and Fe component is an attractive 4 V eco-friendly, low cost cathode material for lithium ion batteries.

Acknowledgment

This work was supported by the International Cooperation of the Korea Institute of Energy Technology Evaluation and Planning (KETEP) grant funded by the Korea government Ministry of Knowledge Economy (No.20128510010050).

References

[1] V. Aravindan, J. Gnanaraj, Y.-S. Lee, S. Madhavi, LiMnP.O4 – a next generation cathode material for lithium-ion batteries, Journal of Materials Chemistry A 1 (2013) 3518–3539.
[2] M.-H. Kim, H.-S. Shin, D. Shin, Y.-K. Sun, Synthesis and electrochemical properties of $Li[Ni_{0.8}Co_{0.1}Mn_{0.1}]O_2$ and $Li[Ni_{0.8}Co_{0.2}]O_2$ via co-precipitation, Journal of Power Sources 159 (2006) 1328–1333.

[3] N.-S. Choi, Z. Chen, S.A. Freunberger, X. Ji, Y.-K. Sun, K. Amine, G. Yushin, L.F. Nazar, J. Cho, P.G. Bruce, Challenges facing lithium batteries and electrical double-layer capacitors, Angewandte Chemie International Edition 51 (2012) 9994–10024.

[4] M.M. Thackeray, C. Wolverton, E.D. Isaacs, Electrical energy storage for transportation – approaching the limits of, and going beyond, lithium-ion batteries, Energy & Environmental Science 5 (2012) 7854–7863.

[5] J. Goodenough, Rechargeable batteries: challenges old and new, Journal of Solid State Electrochemistry 16 (2012) 2019–2029.

[6] Y. Nishi, The development of lithium ion secondary batteries, The Chemical Record 1 (2001) 406–413.

[7] H. Liu, Y. Yang, J. Zhang, Reaction mechanism and kinetics of lithium ion battery cathode material $LiNiO_2$ with CO_2, Journal of Power Sources 173 (2007) 556–561.

[8] M.M. Thackeray, A. de Kock, W.I.F. David, Synthesis and structural characterization of defect spinels in the lithium-manganese-oxide system, Materials Research Bulletin 28 (1993) 1041–1049.

[9] B. Ammundsen, J. Desilvestro, T. Groutso, D. Hassell, J.B. Metson, E. Regan, R. Steiner, P.J. Pickering, Formation, structural properties of layered $LiMnO_2$ cathode materials, Journal of the Electrochemical Society 147 (2000) 4078–4082.

[10] S.K. Martha, H. Sclar, Z. Szmuk Framowitz, D. Kovacheva, N. Saliyski, Y. Gofer, P. Sharon, E. Golik, B. Markovsky, D. Aurbach, A comparative study of electrodes comprising nanometric and submicron particles of $LiNi_{0.50}Mn_{0.50}O_2$, $LiNi_{0.33}Mn_{0.33}Co_{0.33}O_2$, and $LiNi_{0.40}Mn_{0.40}Co_{0.20}O_2$ layered compounds, Journal of Power Sources 189 (2009) 248–255.

[11] A.D. Robertson, P.G. Bruce, The origin of electrochemical activity in Li_2MnO_3, Chemical Communications (2002) 2790–2791.

[12] B. Ammundsen, J. Paulsen, Novel lithium-ion cathode materials based on layered manganese oxides, Advanced Materials 13 (2001) 943–956.

[13] M.M. Thackeray, S.-H. Kang, C.S. Johnson, J.T. Vaughey, R. Benedek, S.A. Hackney, Li_2MnO_3-stabilized $LiMO_2$ (M = Mn, Ni, Co) electrodes for lithium-ion batteries, Journal of Materials Chemistry 17 (2007) 3112–3125.

[14] Z. Lu, J.R. Dahn, In situ and ex situ XRD investigation of $Li[Cr_xLi_{1/3-x/3}Mn_{2/3-2x/3}]O_2$ ($x = 1/3$) cathode material, Journal of the Electrochemical Society 150 (2003) A1044–A1051.

[15] S.-H. Kang, C.S. Johnson, J.T. Vaughey, K. Amine, M.M. Thackeray, The effects of acid treatment on the electrochemical properties of 0.5 Li_2MnO_3 0.5 $LiNi_{0.44}Co_{0.25}Mn_{0.31}O_2$ electrodes in lithium cells, Journal of the Electrochemical Society 153 (2006) A1186–A1192.

[16] Y. Sun, C. Ouyang, Z. Wang, X. Huang, L. Chen, Effect of co content on rate performance of $LiMn_{0.5-x}Co_{2x}Ni_{0.5-x}O_2$ cathode materials for lithium-ion batteries, Journal of the Electrochemical Society 151 (2004) A504–A508.

[17] J.G. Li, J.J. Li, J. Luo, L. Wang, X.M. He, Recent advances in the $LiFeO_2$-based materials for Li-ion batteries, International Journal of Electrochemical Science 6 (2011) 1550–1561.

[18] A.K. Padhi, K.S. Nanjundaswamy, J.B. Goodenough, Phospho-olivines as positive-electrode materials for rechargeable lithium batteries, Journal of the Electrochemical Society 144 (1997) 1188–1194.

[19] M. Tabuchi, A. Nakashima, H. Shigemura, K. Ado, H. Kobayashi, H. Sakaebe, H. Kageyama, T. Nakamura, M. Kohzaki, A. Hirano, R. Kanno, Synthesis, cation distribution, and electrochemical properties of Fe-substituted Li_2MnO_3 as a novel 4 V positive electrode material, Journal of the Electrochemical Society 149 (2002) A509–A524.

[20] M. Tabuchi, Y. Nabeshima, T. Takeuchi, K. Tatsumi, J. Imaizumi, Y. Nitta, Fe content effects on electrochemical properties of Fe-substituted Li_2MnO_3 positive electrode material, Journal of Power Sources 195 (2010) 834–844.

[21] M. Tabuchi, Y. Nabeshima, T. Takeuchi, H. Kageyama, K. Tatsumi, J. Akimoto, H. Shibuya, J. Imaizumi, Synthesis and electrochemical characterization of Fe and Ni substituted Li_2MnO_3 – an effective means to use Fe for constructing Co-free Li_2MnO_3 based positive electrode material, Journal of Power Sources 196 (2011) 3611–3622.

[22] K. Karthikeyan, S. Amaresh, G.W. Lee, V. Aravindan, H. Kim, K.S. Kang, W.S. Kim, Y.S. Lee, Electrochemical performance of cobalt free, $Li_{1.2}(Mn_{0.32}Ni_{0.32}Fe_{0.16})O_2$ cathodes for lithium batteries, Electrochimica Acta 68 (2012) 246–253.

[23] S. Lai, C. Hu, Y. Li, D. Luo, M. Cao, Z. Yu, H. Liu, Preparation and properties of $LiNi_{0.5}Mn_{0.5}O_2$ thin films by spin-coating for lithium micro-batteries, Solid State Ionics 179 (2008) 1754–1757.

[24] P.S. Whitfield, S. Niketic, I.J. Davidson, Effects of synthesis on electrochemical, structural and physical properties of solution phases of Li_2MnO_3–$LiNi_{1-x}Co_xO_2$, Journal of Power Sources 146 (2005) 617–621.

[25] T. Ohzuku, Y. Makimura, Layered lithium insertion material of $LiNi_{1/2}Mn_{1/2}O_2$: a possible alternative to $LiCoO_2$ for advanced lithium-ion batteries, Chemistry Letters (2001) 744–745.

[26] Z. Lu, L.Y. Beaulieu, R.A. Donaberger, C.L. Thomas, J.R. Dahn, Synthesis, structure and electrochemical behavior of $Li[Ni_xLi_{1/3-2x/3}Mn_{2/3-x/3}]O_2$, Journal of the Electrochemical Society 149 (2002) A778–A791.

[27] T. Ohzuku, A. Ueda, M. Nagayama, Electrochemistry and structural chemistry of $LiNiO_2$ (R3m) for 4 volt secondary lithium cells, Journal of the Electrochemical Society 140 (1993) 1862–1870.

[28] C. Julien, M.A. Camacho-Lopez, T. Mohan, S. Chitra, P. Kalyani, S. Gopukumar, Combustion synthesis and characterization of substituted lithium cobalt oxides in lithium batteries, Solid State Ionics 135 (2000) 241–248.

[29] C. Julien, Local cationic environment in lithium nickel–cobalt oxides used as cathode materials for lithium batteries, Solid State Ionics 136–137 (2000) 887–896.

[30] R. Vasanthi, I. RuthMangani, S. Selladurai, Synthesis and characterization of non-stoichiometric compound $LiCo_{1-x-y}Mg_xAl_yO_2$ ($0.03 \le x$ and $y \le 0.07$) for lithium battery application, Inorganic Chemistry Communications 6 (2003) 953–957.

[31] J.W. Fergus, Recent developments in cathode materials for lithium ion batteries, Journal of Power Sources 195 (2010) 939–954.

[32] S.H. Kang, J. Kim, M.E. Stoll, D. Abraham, Y.K. Sun, K. Amine, Layered $Li(Ni_{0.5-x}Mn_{0.5-x}M_{2x'})O_2$ (M′ = Co, Al, Ti; $x = 0$, 0.025) cathode materials for Li-ion rechargeable batteries, Journal of Power Sources 112 (2002) 41–48.

[33] N. Yabuuchi, K. Yoshii, S.-T. Myung, I. Nakai, S. Komaba, Detailed studies of a high-capacity electrode material for rechargeable batteries, Li_2MnO_3–$LiCo_{1/3}Ni_{1/3}Mn_{1/3}O_2$, Journal of the American Chemical Society 133 (2011) 4404–4419.

[34] F. Wu, M. Wang, Y. Su, L. Bao, S. Chen, A novel method for synthesis of layered $LiNi_{1/3}Mn_{1/3}Co_{1/3}O_2$ as cathode material for lithium-ion battery, Journal of Power Sources 195 (2010) 2362–2367.

[35] J. Kim, P. Fulmer, A. Manthiram, Synthesis of $LiCoO_2$ cathodes by an oxidation reaction in solution and their electrochemical properties, Materials Research Bulletin 34 (1999) 571–579.

[36] K.M. Shaju, G.V. Subba Rao, B.V.R. Chowdari, EIS and GITT studies on oxide cathodes, O_2-$Li_{(2/3)+x}(Co_{0.15}Mn_{0.85})O_2$ ($x = 0$ and 1/3), Electrochimica Acta 48 (2003) 2691–2703.

[37] C.S. Johnson, N. Li, J.T. Vaughey, S.A. Hackney, M.M. Thackeray, Lithium-manganese oxide electrodes with layered-spinel composite structures $xLi_2MnO_3 \cdot (1-x)Li_{1+y}Mn_{2-y}O_4$ ($0 < x < 1$, $0 \le y \le 0.33$) for lithium batteries, Electrochemistry Communications 7 (2005) 528–536.

[38] M. Tabuchi, A. Nakashima, K. Ado, H. Sakaebe, H. Kobayashi, H. Kageyama, K. Tatsumi, Y. Kobayashi, S. Seki, A. Yamanaka, The effects of preparation condition and dopant on the electrochemical property for Fe-substituted Li_2MnO_3, Journal of Power Sources 146 (2005) 287–293.

[39] N. Kumagai, J.-M. Kim, S. Tsuruta, Y. Kadoma, K. Ui, Structural modification of $Li[Li_{0.27}Co_{0.20}Mn_{0.53}]O_2$ by lithium extraction and its electrochemical property as the positive electrode for Li-ion batteries, Electrochimica Acta 53 (2008) 5287–5293.

[40] A.D. Robertson, P.G. Bruce, Mechanism of electrochemical activity in Li_2MnO_3, Chemistry of Materials 15 (2003) 1984–1992.

[41] K. Shizuka, T. Kobayashi, K. Okahara, K. Okamoto, S. Kanzaki, R. Kanno, Characterization of $Li_{1+y}Ni_xCo_{1-2x}Mn_xO_2$ positive active materials for lithium ion batteries, Journal of Power Sources 146 (2005) 589–593.

[42] B. Ammundsen, J. Paulsen, I. Davidson, R.-S. Liu, C.-H. Shen, J.-M. Chen, L.-Y. Jang, J.-F. Lee, Local structure and first cycle redox mechanism of layered $Li_{1.2}Cr_{0.4}Mn_{0.4}O_2$ cathode material, Journal of the Electrochemical Society 149 (2002) A431–A436.